in: Proc. EMBC-2015, 37th Annual Intl. Conf. of the IEEE EMBS, Milan, Italy, Aug. 25-29, 2015, pp. 6987-6990.

Atrial Signal Extraction in Atrial Fibrillation Electrocardiograms Using a Tensor Decomposition Approach

Lucas N. Ribeiro[1], Antonio R. Hidalgo-Muñoz[2] and Vicente Zarzoso[2]

***Abstract*— Atrial fibrillation (AF) is the most common cardiac arrhythmia encountered in clinical practice and remains a major challenge in cardiology. The noninvasive analysis of AF usually requires the estimation of the atrial activity (AA) signal in surface electrocardiogram (ECG) recordings. The present contribution puts forward a tensor decomposition approach for noninvasive AA extraction in AF ECG recordings. As opposed to the matrix approach, tensor decompositions are generally unique under mild conditions and have the potential to perform source separation in scenarios with a limited number of electrodes. An experimental study on a synthethic signal model and a real AF ECG recording evaluates the performance of the so-called block term tensor decomposition approach as compared to matrix techniques such as principal component analysis and independent component analysis.**

***Index Terms*— Atrial fibrillation, blind source separation, electrocardiogram, independent component analysis, tensor decompositions.**

I. INTRODUCTION

Atrial fibrillation (AF) is the most prevalent sustained cardiac arrhythmia in the adult population. It consists in a disorganized electrical activation of the atria, caused by ectopic impulses typically originating around the pulmonary veins and reentrant pathways along regions with reduced refractoriness due to substrate remodeling. This abnormal electrical activation is linked to an ineffective atrial contraction, thus increasing the risk of blood clot formation and stroke. In the surface electrocardiogram (ECG), the P-wave of normal atrial activation is replaced by rapid fibrillatory waves (f-waves) during AF, which are masked in time and frequency by ventricular activity (VA) during ventricular beats.

An accurate atrial activity (AA) estimation is an important step for AF analysis [1]. When multiple spatially separated electrodes are available, blind source separation (BSS) techniques can be applied. The BSS approach aims at estimating and isolating signal sources solely linked to atrial activation, and usually rely on matrix decompositions, which require strong mathematical constraints over its factors to assure uniqueness of the decomposition. Constraints such as mutual orthogonality between spatial factors, as in principal component analysis (PCA) [2], and statistical independence between source components, as in independent component analysis (ICA) [3], [4], sometimes do not hold in practical settings or may lack physiological interpretation. Moreover, PCA and ICA are statistical approaches, typically requiring sufficient sample size to work effectively. As the rank of a matrix is limited by its smallest dimension, matrix-based BSS methods cannot deal with the challenging underdetermined scenario, where there are fewer leads than sources.

Tensor decompositions are a promising tool overcoming the above limitations [5]. Higher-order tensors are multidimensional arrays that can be seen as the generalization of usual matrices to more than two dimensions. Among their attractive properties, tensors can be uniquely decomposed under relatively mild conditions and their rank can exceed their dimensions [5], thus allowing the development of more robust BSS methods in limited spatial diversity conditions.

Classical tensor techniques such as the canonical polyadic decomposition (CPD) have already been employed in electroencephalogram (EEG) data for space-time-frequency analysis during epileptic seizures [6] and source localization [7]. More recently, the so-called block term decomposition (BTD) [8] has also been applied to epileptic seizure analysis from the EEG [9]. In the area of cardiac signal processing, tensors have been used for feature extraction and ECG classification [10], as well as fetal ECG extraction from maternal skin recordings during pregnancy [11]. To our knowledge, the application of tensor decompositions to AF analysis remains unexplored.

The present contribution explores the application of tensor decompositions to noninvasive AA extraction in AF ECGs. After recalling the CPD, we show the suitability of BTD in this biomedical context by virtue of the atrial signal characteristics during AF. Finally, a preliminary comparative performance evaluation using a synthetic signal model and real ECG recordings is carried out to gauge the potential benefits from the tensor approach.

II. MATRIX DECOMPOSITION APPROACH TO NONINVASIVE AA EXTRACTION IN AF ECGS

When observing multiple ECG leads, the AA extraction problem can be modeled from the perspective of BSS based on instantaneous linear mixtures [3], [4]. This approach relies on the signal model:

$$\mathbf{Y} = \mathbf{M}\mathbf{S} \tag{1}$$

where $\mathbf{Y} \in \mathbb{R}^{K \times N}$ is the observed ECG data matrix composed of K leads and N samples, $\mathbf{M} \in \mathbb{R}^{K \times R}$ is the mixing matrix and $\mathbf{S} \in \mathbb{R}^{R \times N}$ is the source matrix with

[1]Lucas N. Ribeiro is with Federal University of Ceará, Fortaleza, Brazil nogueira@gtel.ufc.br

[2]Antonio R. Hidalgo-Muñoz and Vicente Zarzoso are with the I3S Laboratory, University of Nice Sophia Antipolis, France {hidalgo, zarzoso}@i3s.unice.fr

Lucas N. Ribeiro is supported by CNPq/CAPES (Brazil). Antonio R. Hidalgo-Muñoz is supported by a Postdoctoral Research Fellowship awarded by the University of Nice Sophia Antipolis. Vicente Zarzoso is a member of the *Institut Universitaire de France*.

R sources. The coefficients of $\mathbf{M}$ reflect the propagation characteristics of cardiac signals from the heart to the body surface, and $\mathbf{S}$ contain the ventricular, atrial and noise sources [3]. BSS methods seek to recover $\mathbf{S}$ and possibly $\mathbf{M}$ knowing only $\mathbf{Y}$. Because this inverse problem is ill-posed, the set of possible solutions must be reduced by exploiting *a priori* knowledge on the sources and/or the mixing system. During AF, atrial and ventricular sources can be considered statistically independent, since atrial wavefronts cause ventricular depolarizations at irregular intervals, thus enabling the application of ICA techniques [3].

III. Tensor Decompositions

A. Canonical Polyadic Decomposition (CPD)

Tensor decompositions have been widely used in space-time-frequency (STF) tensor analysis, obtained by calculating the short-time Fourier transform (STFT) of each sensor signal and concatenating the result in a third-order tensor. CPD has been successfully used for removing artifacts [6] and providing accurate spatial information on STF EEG tensors.

The CPD of a third-order STF tensor $\mathcal{T} \in \mathbb{R}^{I_1 \times I_2 \times I_3}$ is defined as the following sum of rank-1 terms $\mathcal{T} = \sum_{r=1}^{R} \mathbf{m}_r \circ \mathbf{n}_r \circ \mathbf{p}_r$, where $\circ$ denotes the outer product and $\mathbf{m}_r \in \mathbb{R}^{I_1}$, $\mathbf{n}_r \in \mathbb{R}^{I_2}$ and $\mathbf{p}_r \in \mathbb{R}^{I_3}$ are the space, time and frequency signatures of the rth component, respectively. Obtaining the CPD for STF analysis requires the selection of the window length and time delay for STFT computation, as well as numerical algorithms able to cope with complex-valued data. Although these are not serious limitations, the lack of priors in the CPD model makes it difficult to target specific sources of interest. For this reason, we search for alternative decompositions making explicit use of the desired signal characteristics.

B. Block Term Decomposition (BTD)

1) Source model: The AA during AF reflects in the ECG as a narrowband signal. Therefore, modeling it as a sum of complex exponentials is a plausible hypothesis. According to this assumption, the rth atrial source could be expressed as the L_r-pole model:

$$s_{r,n} = \sum_{\ell_r=1}^{L_r} \lambda_{\ell_r,r} z_{\ell_r,r}^{n-1}, \quad 1 \leq n \leq N, 1 \leq r \leq R \tag{2}$$

where L_r is the number of exponential terms, $\lambda_{\ell_r,r}$ is the linear coefficient and $z_{\ell_r,r}$ is the base of the exponential associated with the ℓ_rth term of $s_{r,n}$, also called a pole; symbol n represents the discrete time index. BTD explicitly exploits the source model (2) to perform deterministic BSS, even in the undertermined scenario, under rather general conditions that are summarized next [8].

2) General BTD formulation: The BTD of a third-order data tensor $\mathcal{T}$ is defined as

$$\mathcal{T} = \sum_{r=1}^{R} \mathbf{E}_r \circ \mathbf{c}_r \tag{3}$$

where $\mathbf{E}_r \in \mathbb{R}^{I_1 \times I_2}$ has rank L_r and $\mathbf{c}_r \in \mathbb{R}^{I_3}$. If $\mathbf{E}_r$ admits a decomposition $\mathbf{E}_r = \mathbf{D}_r^{(1)} \mathbf{D}_r^{(2)^T}$, where $\mathbf{D}_r^{(1)} \in \mathbb{R}^{I_1 \times L_r}$ and $\mathbf{D}_r^{(2)} \in \mathbb{R}^{I_2 \times L_r}$ have rank L_r and $(\cdot)^T$ denotes the transpose operator. In view of this, (3) can be expressed as

$$\mathcal{T} = \sum_{r=1}^{R} \left(\mathbf{D}_r^{(1)} \mathbf{D}_r^{(2)^T} \right) \circ \mathbf{c}_r. \tag{4}$$

Note that the rth term of eqn. (4) has multilinear rank $(L_r, L_r, 1)$. This decomposition is unique up to permutation and scaling provided the two following conditions [8]: C1) Factors $\mathbf{D}^{(1)} = [\mathbf{D}_1^{(1)}, \mathbf{D}_2^{(1)}, \ldots, \mathbf{D}_R^{(1)}]$ and $\mathbf{D}^{(2)} = [\mathbf{D}_1^{(2)}, \mathbf{D}_2^{(2)}, \ldots, \mathbf{D}_R^{(2)}]$ are full column rank and, C2) matrix $\mathbf{C} = [\mathbf{c}_1, \mathbf{c}_2, \ldots, \mathbf{c}_R]$ does not contain colinear columns. Note that $I_1, I_2 \geq \sum_{r=1}^{R} L_r$ to satisfy the first condition.

3) Generating the tensor: To obtain a third-order tensor $\mathcal{Y}$ from the observed data matrix $\mathbf{Y}$ while exploiting the narrowband signal model (2), the kth row of $\mathbf{Y}$ is mapped on to a $(I \times J)$ Hankel matrix, which we denote $\mathbf{H}_{\mathbf{Y}}^{(k)}$, and stored in the kth matrix slice of $\mathcal{Y}$:

$$[\mathcal{Y}]_{:,:,k} = \mathbf{H}_{\mathbf{Y}}^{(k)}. \tag{5}$$

Due to the Hankel structure, dimensions I and J fulfil $I + J - 1 = N$, and, to maximize the resulting matrix rank, are chosen as $I = J = \frac{N+1}{2}$ if N is odd, or $I = \frac{N}{2}$ and $J = \frac{N}{2} + 1$ if N is even. This procedure yields a tensor $\mathcal{Y}$ with dimensions $I \times J \times K$.

According to this structure and observation model (1), the entries of tensor $\mathcal{Y}$ can be expressed as $[\mathcal{Y}]_{i,j,k} = \sum_{r=1}^{R} m_{k,r} s_{r,i+j-1}$ in which $m_{k,r}$ and $s_{r,i+j-1}$ are the (k,r) and $(r, i+j-1)$ entries of $\mathbf{M}$ and $\mathbf{S}$, respectively, for $1 \leq i \leq I, 1 \leq j \leq J, 1 \leq k \leq K$. Consequently, the kth matrix slice of $\mathcal{Y}$ given in (5) can be expressed as

$$[\mathcal{Y}]_{:,:,k} = \sum_{r=1}^{R} m_{k,r} \mathbf{H}_{\mathbf{S}}^{(r)} \tag{6}$$

where, much in the same fashion as $\mathbf{H}_{\mathbf{Y}}^{(k)}$, notation $\mathbf{H}_{\mathbf{S}}^{(r)}$ stands for the $(I \times J)$ Hankel matrix obtained from the rth row of $\mathbf{S}$. The above equation accepts the tensor formulation:

$$\mathcal{Y} = \sum_{r=1}^{R} \mathbf{H}_{\mathbf{S}}^{(r)} \circ \mathbf{m}_r \tag{7}$$

which is a particular case of the BTD model (3).

4) Uniqueness under source model (2): To understand why the BTD model (3) is unique under source model (2), one just needs to take into account that the associated Hankel matrix $\mathbf{H}_{\mathbf{S}}^{(r)}$ admits a Vandermonde decomposition, and a tall Vandermonde matrix generated by L_r distinct poles has full-column rank L_r. Hence, according to uniqueness conditions C1–C2, model (7) will be unique if all poles $z_{\ell_r,r}$ are distinct, $1 \leq \ell_r \leq L_r$, $1 \leq r \leq R$, and $\mathbf{M}$ does not have proportional columns

From the above theoretical derivations, it follows that BTD would allow the extraction of AA sources during AF even in limited spatial diversity scenarios.

IV. Experimental Assessment

A. Generating Synthetic AF ECG Recordings

1) Synthetic atrial source: In this preliminary performance evaluation, we adopt a simplified atrial source model that mimics the sawtooth pattern typically characterizing the AA signal in early forms of AF or in more organized supraventricular arrhythmias like atrial flutter:

$$f_n = -\sum_{i=1}^{M} \frac{2a}{i\pi} \sin\left(\frac{2\pi i f_0}{F_s} n\right) \tag{8}$$

where a is the sawtooth amplitude, f_0 the dominant frequency and F_s the sampling rate. This expression can be derived from the more general model proposed in [12], but without amplitude and frequency modulation. Since one sinusoid consists of two conjugated exponentials, the synthetic f-wave (8) will consist of $2M$ exponentials in this case, a relation that facilitates the parameter selection of BTD. Indeed, recall that symbol L_r denotes the number of poles that generate the rth source, which is also rank $\left(\mathbf{H}_{\mathbf{S}}^{(r)}\right)$ (Sec. III-B). Hence, under model (8), we have $L_r = 2M$.

2) Synthetic AF ECG: Synthetic AF ECGs are generated by superposing synthetic f-waves generated by the above model to a real ECG signal from a healthy subject after P-wave suppression. The ECG is obtained from the PTB diagnostic database [13]. This ECG, acquired at a sampling rate of 1 kHz, is preprocessed using a forward-backward bandpass type-II Chebyshev IIR filter with cut-off frequencies of 0.5 Hz and 30 Hz to remove baseline wander and powerline interference. P-waves are manually segmented and then suppressed by spline interpolation between their onset and offset points. The resulting signals, representing the VA, are stored after power normalization in matrix $\mathbf{V} \in \mathbb{R}^{L\times N}$, where L denotes the number of leads and N the number of samples. The synthetic AA signal is generated according to (8) and stored in vector $\mathbf{f} \in \mathbb{R}^N$. After power normalization, the AA is defined as $\mathbf{A} = \mathbf{a}\mathbf{f}^T \in \mathbb{R}^{L\times N}$, where $\mathbf{a} \in \mathbb{R}^L$ is a random vector which represents the atrial spatial signature. A normalized white Gaussian noise component $\mathbf{B}$ is also considered to model sensor noise. The synthetic AF ECG data matrix $\mathbf{Y}$ is finally given by

$$\mathbf{Y} = \mathbf{V} + \gamma\mathbf{A} + \sigma\mathbf{B} \tag{9}$$

where γ and σ are the power factors of the atrial and noise components, respectively. We define the atrial-ventricular ratio (AVR) as AVR $= \gamma^2$ and the signal-to-noise ratio (SNR) as SNR $= \gamma^2/\sigma^2$.

B. Extraction Performance in Synthetic Recordings

A synthetic AF signal is generated according to model (8) with $M = 5$ harmonics, $f_0 = 6$ Hz and sampling rate of $F_s = 1$ kHz. The sawtooth amplitude a becomes irrelevant after power normalization, and is then absorbed by the atrial power factor γ in (9). The AVR is set to -3 dB. After generating the observation tensor as explained in Sec. III-B, its BTD is computed by fixing $R = 4$ and $L_r = 2M = 10$, $r = 1, 2, 3, 4$. The BTD factors are randomly initialized, and the decomposition is computed using the MATLAB implementation [14] of the nonlinear least-squares (NLS) approach proposed in [15]. The absolute value of the Pearson correlation coefficient between the generated and the estimated f-wave signal is used as performance index. Monte Carlo (MC) simulations with 30 independent runs are conducted to obtain a performance index for each method in a given scenario. Each MC run consists in generating a noisy AF ECG, extracting the synthetic f wave and calculating the correlation between the estimated and the generated f wave. After the MC runs, the mean correlation is calculated for each method. The results by BTD are compared to those by two BSS methods based on matrix decompositions, namely, PCA [2] and RobustICA-f [4].

1) Robustness to additive white Gaussian noise: Figure 1 summarizes the performance of the three techniques for varying SNR, with $N = 5000$ samples and $L = 4$ leads (V1-V4). Clearly, BTD consistently offers a superior performance, especially in the low SNR range.

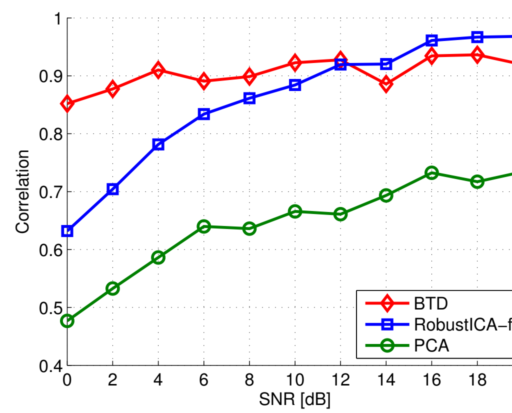

Fig. 1. Extraction performance for varying SNR, with $N = 5000$ samples and $L = 4$ leads (V1-V4).

2) Robustness to reduced sample size: The impact of sample size on estimation quality is shown in Fig. 2, obtained with leads V1-V4 at 0-dB SNR. BTD outperforms the matrix techniques except in very short observation windows, which is somewhat unexpected in a deterministic technique like the tensor decomposition considered in this work.

3) Robustness to limited spatial diversity: Fig. 3 displays the performance variations with the number of leads. BTD offers again a consistently superior performance, even using as few as two leads only.

C. Illustrative Real AF ECG Recording

To validate the applicability of BTD in a clinical context, an additional experiment is conducted with a real AF ECG observation acquired from a patient suffering from persistent AF. The original recording is composed of $N = 1000$ samples of $L = 4$ leads, of which only V1 is shown in Fig. 4. Although the BTD parameters were obtained by trial and error in this example, the tensor technique yields an f-wave estimate much closer to the actual atrial signal present in

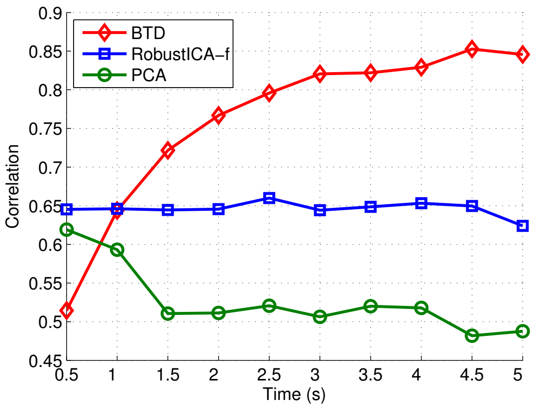

Fig. 2. Extraction performance for varying sample size, with SNR = 0 dB and $L = 4$ leads (V1-V4).

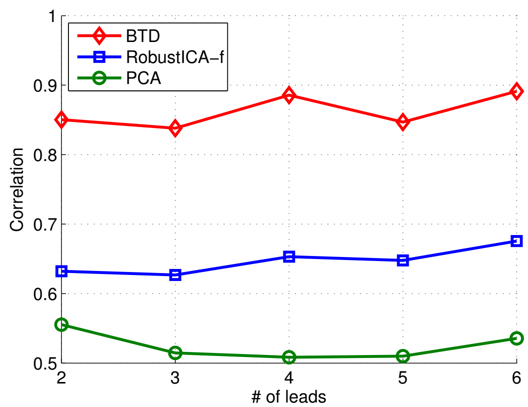

Fig. 3. Extraction performance for varying number of leads, with $N = 5000$ samples and SNR = 0 dB.

the recording. Remark that the ECG recordings analyzed in these experiments would be too short for beat subtraction algorithms to perform properly.

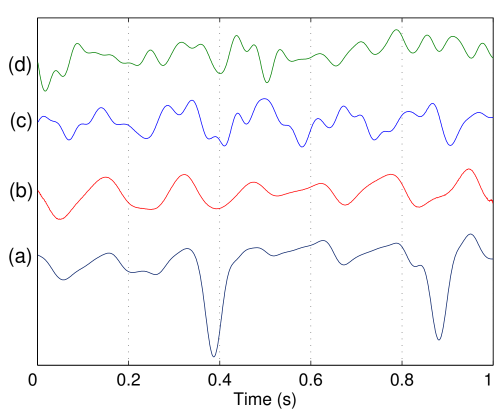

Fig. 4. Results on an illustrative real AF ECG recording. (a) Lead V1 of the original recording, consisting of 1000 samples. Estimated AA from BTD (b), RobustICA-f (c) and PCA (d). The three methods are applied on $L = 4$ leads (V1-V4); BTD is computed using $R = 3$ and $L_r = 48$, $r = 1, 2, 3$.

V. Conclusions

With the goal of overcoming the drawbacks of matrix-based BSS methods, this work has approached for the first time the problem of noninvasive AA extraction during AF from the perspective of tensor decompositions. Using a simple atrial signal model and a real AF ECG recording, numerical experiments demonstrate that BTD outperforms matrix-based methods in noisy and spatially-constrained scenarios. Further research should aim at understanding the unexpected performance deterioration of the tensor technique for short observation windows, designing automatic parameter selection methods for BTD, and evaluating its performance in more realistic AF signal models.

References

[1] L. Mainardi, L. Sornmo, and S. Cerutti, *Understanding atrial fibrillation: the signal processing contribution*. Morgan & Claypool Publishers, 2008.

[2] D. Raine, P. Langley, A. Murray, A. Dunuwille, and J. P. Bourke, "Surface atrial frequency analysis in patients with atrial fibrillation," *Journal of cardiovascular electrophysiology*, vol. 15, no. 9, pp. 1021–1026, 2004.

[3] J. J. Rieta, F. Castells, C. Sánchez *et al.*, "Atrial activity extraction for atrial fibrillation analysis using blind source separation," *IEEE Transactions on Biomedical Engineering*, vol. 51, no. 7, pp. 1176–1186, 2004.

[4] V. Zarzoso and P. Comon, "Robust independent component analysis by iterative maximization of the kurtosis contrast with algebraic optimal step size," *IEEE Trans Neural Netw*, vol. 21, no. 2, pp. 248–261, 2010.

[5] T. G. Kolda and B. W. Bader, "Tensor decompositions and applications," *SIAM review*, vol. 51, no. 3, pp. 455–500, 2009.

[6] E. Acar, C. Aykut-Bingol, H. Bingol *et al.*, "Multiway analysis of epilepsy tensors," *Bioinformatics*, vol. 23, no. 13, pp. 10–18, 2007.

[7] H. Becker, L. Albera, P. Comon *et al.*, "EEG extended source localization: tensor-based vs. conventional methods," *NeuroImage*, vol. 96, pp. 143–157, 2014.

[8] L. De Lathauwer, "Blind separation of exponential polynomials and the decomposition of a tensor in rank-$(L_r, L_r, 1)$ terms," *SIAM Journal on Matrix Analysis and Applications*, vol. 32, no. 4, pp. 1451–1474, 2011.

[9] B. Hunyadi, D. Camps, L. Sorber *et al.*, "Block term decomposition for modelling epileptic seizures," *EURASIP Journal on Advances in Signal Processing*, vol. 2014, no. 1, pp. 1–19, 2014.

[10] K. Huang and L. Zhang, "Cardiology knowledge-free ECG feature extraction using generalized tensor rank one discriminant analysis," *EURASIP Journal on Advances in Signal Processing*, vol. 2014, no. 1, pp. 1–15, 2014.

[11] M. Niknazar, H. Becker, B. Rivet *et al.*, "Robust 3-way tensor decomposition and extended state Kalman filtering to extract fetal ECG," in *Proceedings of the 21st European Signal Processing Conference (EUSIPCO), Marrakech, Morocco*, Sept 2013.

[12] M. Stridh and L. Sörnmo, "Spatiotemporal QRST cancellation techniques for analysis of atrial fibrillation," *IEEE Transactions on Biomedical Engineering*, vol. 48, no. 1, pp. 105–111, 2001.

[13] A. L. Goldberger, L. A. N. Amaral, L. Glass *et al.*, "Physiobank, physiotoolkit, and physionet components of a new research resource for complex physiologic signals," *Circulation*, vol. 101, no. 23, pp. e215–e220, 2000.

[14] L. Sorber, M. V. Barel, and L. D. Lathauwer, "Tensorlab v2.0," *Available online, January 2014. URL: http://www.tensorlab.net/.*

[15] L. Sorber, M. Van Barel, and L. De Lathauwer, "Optimization-based algorithms for tensor decompositions: Canonical polyadic decomposition, decomposition in rank-$(L_r, L_r, 1)$ terms, and a new generalization," *SIAM Journal on Optimization*, vol. 23, no. 2, pp. 695–720, 2013.